JCTC Journal of Chemical Theory and Computation

Article

pubs.acs.org/JCTC

Electronic and Vibrational Nonlinear Optical Properties of Five Representative Electrides

Marc Garcia-Borràs,[†] Miquel Solà,[†] Josep M. Luis,*[,†] and Bernard Kirtman[‡]

[†]Institut de Química Computacional and Departament de Química, Universitat de Girona, Campus Montilivi, 17071 Girona, Catalonia, Spain

[‡]Department of Chemistry and Biochemistry, University of California, Santa Barbara, California 93106, United States

Supporting Information

ABSTRACT: The electrides have a very special electronic structure with diffuse excess electrons not localized on any specific atom. Such systems are known to have huge electronic nonlinear optical (NLO) properties. Here, we determine and analyze the vibrational, as compared to the electronic, NLO properties for a representative set of electrides: Li@Calix, Na@Calix, Li@$B_{10}H_{14}$, $Li_2^{\bullet+}TCNQ^{\bullet-}$, and $Na_2^{\bullet+}TCNQ^{\bullet-}$. The static and dynamic vibrational (hyper)polarizabilities are computed by the nuclear relaxation method (with field-induced coordinates and the infinite optical frequency approximation) at the UB3LYP level using a hybrid Pople basis set. In general, the static vibrational β_{vec} and $\gamma_{\parallel}$ exceed the corresponding static electronic property values by up to an order of magnitude. The same comparison for dynamic vibrational hyperpolarizabilities shows a smaller ratio. For the intensity-dependent refractive index (IDRI) and dc-Kerr processes, the ratio is on the order of unity or somewhat larger; it is less for the dc-Pockels and the electric field induced second harmonic (EFISH) effects (as well as the static $\bar{\alpha}$) but still important. The role of anharmonicity, motion of the alkali atoms, and substitution of Na for Li is discussed along with specific aspects of the charge distribution associated with the excess electron.

1. INTRODUCTION

Electrides are ionic compounds in which electrons behave as anions.[1] These special electrons are not localized on specific atoms or bonds but rather are separated from any nuclei, occupying positions typically populated by anions in ionic compounds. Crystalline electrides may be understood as stoichiometric F centers in which all anionic sites contain trapped electrons. Such structures, as well as structures with electride characteristics, can be obtained as alkali atom adducts of organic molecules like cryptands and crown ethers[1d,2] or alkali atom adducts of inorganic molecular sieves like synthetic sodalities and zeolites,[3] or as an inorganic nanoporous single crystal like $[Ca_{24}Al_{28}O_{64}]^{4+}$ $(4e^-)$.[1b,c,4]

As one might anticipate, the electronic distribution in electride-like structures leads to easily polarizable systems with large predicted nonlinear optical properties (NLOP).[5] The diffuse excess electrons play a key role in determining the large magnitude of the first and second hyperpolarizabilities. We focus here on the NLOP of a set of five electride structures formed by alkali atom adducts of organic molecules, i.e., $Li^+(Calix)e^-$ (Li@Calix) (Calix = Calix[4]pyrrole),[5a] $Na^+(Calix)e^-$ (Na@Calix), $Li_2^{\bullet+}TCNQ^{\bullet-}$ (TCNQ = tetracyanoquinodimethane),[5b] $Na_2^{\bullet+}TCNQ^{\bullet-}$,[5b] and an Li adduct of a $B_{10}H_{14}$ borane complexant $(Li@B_{10}H_{14})$[5c] (see Figure 1). In all but the last case, the alkali valence electron is pushed out by repulsive interaction with nitrogen lone pairs, whereas for Li@$B_{10}H_{14}$, the Li valence electron is pulled inward by the four electron-deficient terminal H atoms of the basket-like borane. Due to a loosely bound valence electron provided by the alkali atoms, both types of molecules have a predicted electronic first and second hyperpolarizability that is orders of magnitude larger than the corresponding complexant or the same compound with a positive charge.[5a−c] For instance, the predicted static first hyperpolarizability of $B_{10}H_{14}$, $[Li@B_{10}H_{14}]^+$, and $Li@B_{10}H_{14}$ is 68 au, 100 au, and 23075 au, respectively.[5c] Molecules with high NLOP, such as $Li@B_{10}H_{14}$, are of considerable interest due to potential utilization in a variety of optical and opto-electronic devices.[6]

Using a clamped nucleus approximation,[7] the polarizability and hyperpolarizabilities can be decomposed into electronic and vibrational contributions.[8] The predictions mentioned above have been based on the electronic contribution. However, the effect of vibrations on the hyperpolarizabilities can be quite important and may even be much larger than the electronic counterpart.[9] For that reason, it is important to consider the vibrational contribution when assessing a particular nonlinear optical material.

Bishop and Kirtman (BK) have presented a perturbation treatment[10] (BKPT) that has paved the way for calculating the static and dynamic vibrational hyperpolarizabilities of polyatomic molecules. A simplified computational procedure, known as the nuclear relaxation (NR) approach,[11] was subsequently developed for the most important NLO processes. This general approach is related to BKPT, but it is variational[11a,b] and can be combined either with perturbation theory[12] or one of several variation methods[9b,13] to calculate vibrational NLO properties. When combined with perturbation theory, one can relate the results to the BKPT expressions.[11c,d] However, when BKPT converges slowly or is nonconvergent, the pure variational form is preferred. There is an extension of the original NR method which, in principle, yields the "exact" vibrational NLO

Received: May 29, 2012
Published: July 16, 2012

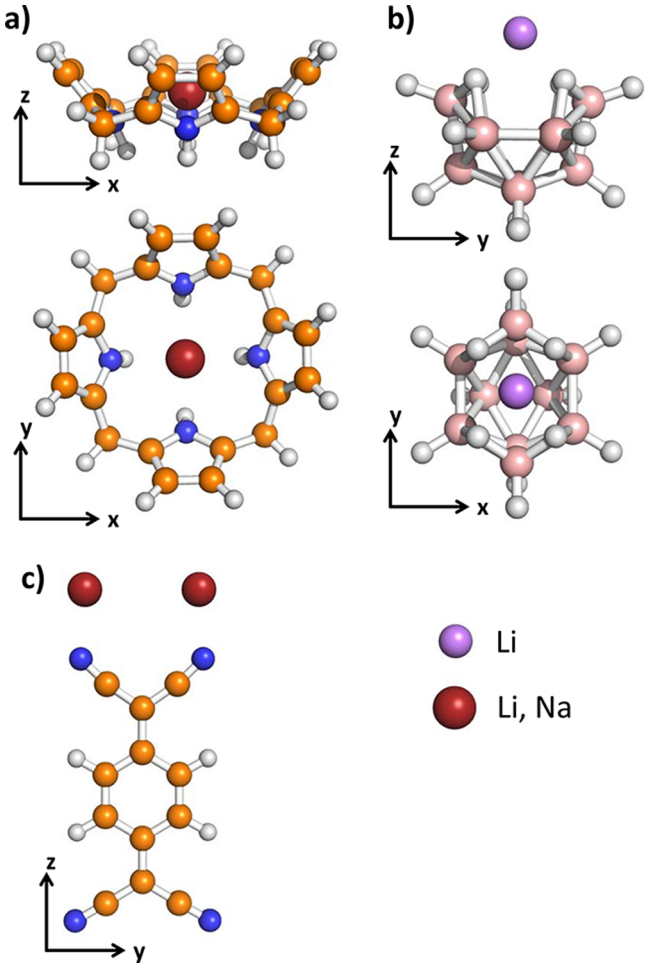

Figure 1. B3LYP/6-31++G(d)/6-311++G(3df) optimized geometries of (a) Li@Calix and Na@Calix, (b) $Li@B_{10}H_{14}$, (c) $Li_2^{\bullet+}TCNQ^{\bullet-}$, and $Na_2^{\bullet+}TCNQ^{\bullet-}$.

properties taking into account all high-order vibrational contributions not otherwise included.[11c] However, these high-order vibrational corrections, which are called curvature contributions, are usually smaller; they are also far more expensive to obtain[12] and are, therefore, not computed here.

The most efficient implementation of the NR method utilizes the infinite optical frequency (IOF) approximation for the dynamic properties. This corresponds to assuming that the ratio $(\omega_v/\omega)^2$ is negligible compared to unity when ω is a (external) laser optical frequency and ω_v is a vibrational transition frequency within the ground electronic state. Tests that have been carried out show that the IOF approximation is accurate as long as the optical frequencies are well above the infrared region.[14]

Recently, the response function formalism for electronic molecular properties has been extended to include vibrational properties as well.[13b,d,15] This treatment contains a contribution omitted in the BKPT method (and in the NR approach),[13d] which is associated with the assumption that electronic transition frequencies are much larger than laser optical frequencies when the latter are in the nonresonant regime. However, the *missing* contribution vanishes in the static and IOF limits.[16] The present work pertains to these two limits, and thus, it is satisfactory to apply the simpler NR method.

The main goal of the study presented here is to investigate the magnitude of the vibrational NLO properties of electrides and/or systems with electride characteristics. For this purpose, we have chosen the molecules identified above (see Figure 1) since they have already been shown to have large electronic hyperpolarizabilities.

2. COMPUTATIONAL METHODS

Most calculations were performed at the UB3LYP[17] level using the Gaussian 09 program package.[18] For the alkali-TCNQ salts, we also carried out ROB3LYP calculations on the ground state triplet and obtained very similar results. The UMP2 and ROMP2 methods were also used for testing proposes. Combinations (see section 3) of 6-31G, 6-311G, 6-31+G, 6-311+G, 6-31+G(d), 6-311+G(d), 6-31++G(d), 6-311++G(d), 6-31++G(d,p), 6-311G(d,p), 6-311++G(d,p), and 6-311+G-(3df) Pople basis sets[19] were applied in determining the nonlinear optical properties. B3LYP electronic dipole moments, polarizabilities, and first hyperpolarizabilities were evaluated analytically, whereas the B3LYP second hyperpolarizabilities, as well as MP2 electronic first and second hyperpolarizabilites, were computed as finite field derivatives of an appropriate lower-order (hyper)polarizability. Some vibrational properties, namely the Hessian, dipole derivatives, and polarizability derivatives with respect to normal coordinates were obtained analytically. All remaining higher-order derivatives required to compute the vibrational hyper(polarizabilities) were calculated by numerical differentiation of the highest-order analytical derivative available.

The average (hyper)polarizabilities may be defined by the following equations:[8]

$$\bar{\alpha} = \frac{1}{3}\sum_{i=x,y,z}\alpha_{ii} \tag{1}$$

$$\beta_{vec} = \left(\sum_{i=x,y,z}\beta_i^2\right)^{1/2} \tag{2}$$

with

$$\beta_i = \frac{1}{3}\sum_{j=x,y,z}(\beta_{ijj} + \beta_{jij} + \beta_{jji}) \tag{3}$$

and

$$\gamma_{\parallel} = \frac{1}{15}\sum_{i,j=x,y,z}\gamma_{iijj} + \gamma_{ijij} + \gamma_{ijji} \tag{4}$$

As noted in the Introduction, the static and dynamic vibrational (hyper)polarizabilities were evaluated using the NR approach[11] including the infinite optical frequency (IOF) approximation. The particular implementation utilized here is based on (static) field induced coordinates (FICs).[14c,20] The FICs are derived from the displacement of the field-free normal coordinates induced by a uniform static electric field. This displacement may be expanded as a power series in the field to yield first-order, second-order, etc. FICs depending upon the order of the field. At each order, the FICs may be separated into harmonic and anharmonic components as well (for the first-order FICs, the anharmonic component vanishes). Through second-order, the harmonic component can be obtained analytically. Without FICs, the number of nth-order derivatives with respect to normal coordinates required to evaluate the vibrational (hyper)polarizabilities is on the order of $(3N - 6)^n$, where N is the number of atoms and $n + 1$ is the order of the property (i.e., first-order for the linear polar-

Table 1. Average Electronic Linear Polarizabilities, As Well As First and Second Hyperpolarizabilities, Calculated at the UMP2 and UB3LYP Levels Using a 6-31+G/6-31+G(d) Basis Set for the Five Electride Molecules Shown in Figure 1[a]

properties	methodology	Li@Calix	Na@Calix	Li@$B_{10}H_{14}$	$Li_2^{\bullet+}TCNQ^{\bullet-}$	$Na_2^{\bullet+}TCNQ^{\bullet-}$
$\bar{\alpha}^e(0;0)$	UMP2	390.4	430.0	162.0	316.9	371.4
	UB3LYP	381.6	430.0	150.3	371.9	389.7
$\beta^e_{vec}(0;0,0)$	UMP2	2.13×10^4	1.02×10^4	1.42×10^4	2.28×10^4	2.53×10^4
	UB3LYP	1.04×10^4	6.61×10^3	7.25×10^3	3.65×10^4	2.16×10^4
$\gamma^e_{\parallel}(0;0,0,0)$	UMP2	4.7×10^6	7.5×10^6	1.0×10^6	1.8×10^6	2.4×10^6
	UB3LYP	4.8×10^6	1.0×10^7	4.8×10^5	1.4×10^6	1.3×10^6

[a]The larger 6-31+G(d) basis set is utilized for Li and Na and the smaller 6-31+G basis set for all other atoms. All quantities are in atomic units.

izability, second-order for the first hyperpolarizability, etc.). When FICs are utilized, the number of derivatives is constant, independent of N, and the main bottleneck of the calculations is removed.

Only one first-order FIC is required to calculate each diagonal tensor component of $\alpha^{nr}(0;0)$, $\beta^{nr}(0;0,0)$, $\beta^{nr}(-\omega;\omega,0)_{\omega\to\infty}$ (IOF approximation; dc-Pockels β), and $\gamma^{nr}(-2\omega;\omega,\omega,0)_{\omega\to\infty}$ (IOF approximation; electric field induced second harmonic (EFISH) γ). In addition, one unique FIC—in this case, the harmonic second-order FIC—suffices for each diagonal component of $\gamma^{nr}(-\omega;\omega,-\omega,\omega)_{\omega\to\infty}$ (IOF approximation; intensity-dependent refractive index (IDRI) γ). Just two FICs, the first-order one and the harmonic term of the second-order one, are necessary to obtain each diagonal component of $\gamma^{nr}(-\omega;\omega,0,0)_{\omega\to\infty}$ (IOF approximation; dc-Kerr effect γ).

Finally, the calculation of $\gamma^{nr}(0;0,0,0)$ requires the full second-order FIC instead of just the harmonic part. Since it is very expensive to determine the anharmonic component of the second-order FIC, we use, instead, the numerical finite field NR (i.e., FF-NR) methodology.[21] In the FF-NR methodology, one needs to optimize the geometry in the presence of a finite static field while strictly imposing the Eckart conditions.[22] Then, a finite field numerical differentiation of the electronic energy or dipole moment is carried out, in this case using field strengths of ±0.0001, ±0.0002, ±0.0004, ±0.0008, ±0.0016, ±0.0032, and ±0.0064 au. The smallest magnitude field that produced a stable vibrational NLO property was selected using a Romberg method triangle.[23]

In BKPT square bracket notation,[10c] the nuclear relaxation contributions are given by

$$\alpha^{nr}_{\alpha\beta}(0;0) = [\mu^2]^0_1 \tag{5}$$

$$\beta^{nr}_{\alpha\beta\gamma}(0;0,0) = [\mu\alpha]^0_2 + [\mu^3]^I_2 \tag{6}$$

$$\beta^{nr}_{\alpha\beta\gamma}(-\omega;\omega,0) = [\mu\alpha]^0_1 \tag{7}$$

$$\gamma^{nr}_{\alpha\beta\gamma\delta}(0;0,0,0) = [\alpha^2]^0_3 + [\mu\beta]^0_3 + [\mu^2\alpha]^I_3 + [\mu^4]^{II}_3 \tag{8}$$

$$\gamma^{nr}_{\alpha\beta\gamma\delta}(-\omega;\omega,0,0) = [\alpha^2]^0_2 + [\mu\beta]^0_2 + [\mu^2\alpha]^I_2 \tag{9}$$

$$\gamma^{nr}_{\alpha\beta\gamma\delta}(-2\omega;\omega,\omega,0) = [\mu\beta]^0_1 \tag{10}$$

and

$$\gamma^{nr}_{\alpha\beta\gamma\delta}(-\omega;\omega,-\omega,\omega) = [\alpha^2]^0_{2'} \tag{11}$$

where the upper index on the square bracket indicates the total order of anharmonicity and the lower index is the number of external static fields involved in the definition of the property, i.e., the number of zeroes to the right of the semicolon. Note that we have used the lower index 2′ in eq 11 to indicate that there is a cancellation between + and $-\omega$ that mimics the effect of two static fields). The properties inside the square bracket indicate which derivatives of the electronic property are involved (for instance, $[\mu\beta]^0_2$ contains derivatives of the electronic dipole moment multiplied by derivatives of the first hyperpolarizability).

3. RESULTS AND DISCUSSION

The calculation of vibrational NLO properties is computationally far more demanding than the evaluation of their electronic counterparts. Furthermore, we are interested here in the complete nuclear relaxation contribution which, for the dc-Kerr effect as an example, requires first derivatives of the Hessian as well as first and second derivatives of electrical properties with respect to nuclear coordinates. This means that the use of an *ab initio* high-level correlated wave function, together with a large basis set, is outside of our computational capabilities. Thus, we decided to use a DFT approach with a tailored basis set. Taking into account that the shape of our molecules is such that they are not candidates for the DFT catastrophe,[24] we chose the B3LYP method. Due to the very special shape of the electron density in the electrides, the magnitude of their predicted NLOP can strongly depend upon the level of calculation. Hence, we carefully checked that both the B3LYP method and the chosen basis set lead to reliable results.

As far as the method is concerned, a comparison between the MP2 and B3LYP electronic average (hyper)polarizabilities, computed with a hybrid 6-31+G/6-31+G(d) basis set, is presented in Table 1 (the choice of this hybrid basis is discussed below). In order to properly account for the change in equilibrium geometry, all properties are computed at the equilibrium geometry of the individual molecule obtained with the particular method. As expected, the dependence of the electronic NLOP on the method is larger for the hyperpolarizabilites than for the linear polarizabilities. For the latter, the average absolute difference between MP2 and B3LYP results is 6%, with a maximum of 17% for the linear polarizability of $Li_2^{\bullet+}TCNQ^{\bullet-}$. For the first and second hyperpolarizabilities, the average absolute difference between B3LYP and MP2 is 37%, with a maximum of 60%, which occurs for the first hyperpolarizability of $Li_2^{\bullet+}TCNQ^{\bullet-}$ once again. Thus, for this set of electrides, B3LYP correctly reproduces the electronic NLOP to substantially better than an order of magnitude. For this work, we want to know the relative importance of the vibrational hyperpolarizabilities as compared to their electronic counterparts, and in our judgment the above data show that B3LYP is sufficiently accurate for that purpose. The much greater expense of calculating MP2 vibrational NR properties also weighed significantly in our choice of the B3LYP method.

Table 2. Average Electronic Linear Polarizabilities, As Well As First and Second Hyperpolarizabilities, of Li@Calix Calculated at the UB3LYP Level Using Different Basis Sets and the Optimized UB3LYP/6-311G(d,p) Geometry[a]

Li@Calix	α^e_{xx} (0;0)	α^e_{zz} (0;0)	$\overline{\alpha}^e$(0;0)	β^e_{xxz} (0;0,0)	β^e_{zzz} (0;0,0)	β^e_{vec}(0;0,0)	γ^e_{xxxx} (0;0,0,0)	γ^e_{zzzz} (0;0,0,0)	$\gamma^e_{\|}$ (0;0,0,0)
6-31G	3.337×10^2	2.019×10^2	2.897×10^2	-1.804×10^3	-9.226×10^2	4.531×10^3	2.53×10^5	1.71×10^5	2.48×10^5
6-31G/6-31+G	4.292×10^2	2.827×10^2	3.803×10^2	3.289×10^3	1.243×10^4	1.900×10^4	7.60×10^6	3.57×10^6	6.24×10^6
6-31G/6-311G	3.709×10^2	2.368×10^2	3.262×10^2	-1.363×10^3	2.678×10^2	2.459×10^3	-1.16×10^5	-1.57×10^4	4.97×10^3
6-31+G	3.970×10^2	2.871×10^2	3.604×10^2	2.061×10^3	8.214×10^3	1.233×10^4	4.96×10^6	3.42×10^6	4.79×10^6
6-31+G/ 6-31+G(d)	4.391×10^2	2.893×10^2	3.892×10^2	1.791×10^3	8.398×10^3	1.198×10^4	5.08×10^6	3.46×10^6	4.90×10^6
6-311G	3.910×10^2	2.595×10^2	3.472×10^2	-1.616×10^3	1.047×10^3	2.185×10^3	8.14×10^4	4.62×10^4	2.25×10^5
6-311+G	4.428×10^2	2.998×10^2	3.952×10^2	1.661×10^3	7.945×10^3	1.127×10^4	3.91×10^6	2.45×10^6	3.87×10^6
6-31+G(d)	4.459×10^2	2.950×10^2	3.956×10^2	1.596×10^3	8.557×10^3	1.175×10^4	5.43×10^6	3.69×10^6	5.23×10^6
6-31++G(d)/ 6-311++G(d)	4.511×10^2	3.091×10^2	4.037×10^2	2.100×10^3	8.698×10^3	1.290×10^4	4.97×10^6	2.99×10^6	4.86×10^6
6-31++G(d)	4.524×10^2	3.027×10^2	4.025×10^2	2.939×10^3	8.586×10^3	1.446×10^4	5.47×10^6	3.32×10^6	5.48×10^6
6-31++G(d)/ 6-311+G(3df)	4.546×10^2	3.099×10^2	4.063×10^2	2.338×10^3	9.822×10^3	1.450×10^4	5.49×10^6	3.41×10^6	5.33×10^6
6-311G(d,p)	3.994×10^2	2.672×10^2	3.553×10^2	1.084×10^3	1.084×10^3	3.252×10^3	1.75×10^5	5.02×10^4	2.96×10^5
6-31++G(d,p)	4.545×10^2	3.036×10^2	4.042×10^2	2.887×10^3	8.579×10^3	1.435×10^4	5.50×10^6	3.32×10^6	5.51×10^6
6-311+G(d)	4.491×10^2	3.062×10^2	4.015×10^2	1.545×10^3	8.100×10^3	1.119×10^4	4.11×10^6	2.62×10^6	4.10×10^6
6-311++G(d)	4.509×10^2	3.092×10^2	4.037×10^2	1.988×10^3	9.104×10^3	1.308×10^4	4.75×10^6	3.20×10^6	4.82×10^6
6-311++G(d,p)	4.544×10^2	3.115×10^2	4.068×10^2	1.967×10^3	9.176×10^3	1.311×10^4	4.87×10^6	3.26×10^6	4.95×10^6
6-311++G(d,p)/ 6-311+G(3df)	4.557×10^2	3.118×10^2	4.077×10^2	2.157×10^3	1.011×10^4	1.443×10^4	5.25×10^6	3.64×10^6	5.31×10^6

[a]The unique diagonal components are also presented along with the *xxz* component of β^e. When two basis set are indicated, the larger one is used for Li and the smaller one for all other atoms. All quantities are in atomic units.

Table 3. Diagonal Component of the Electronic and Finite Field Nuclear Relaxation (NR) Contributions to the Static (Hyper)Polarizabilities along the *z* Symmetry Axis Calculated at the UB3LYP Level with the 6-31+G/6-31+G(d), 6-31+G/6-31+G(d), and 6-31++G(d)/6-311++G(3df) Hybrid Basis Sets for the Five Electride Molecules Shown in Figure 1[a]

properties	Li@Calix	Na@Calix	Li@$B_{10}H_{14}$	$Li_2^{\bullet+}TCNQ^{\bullet-}$	$Na_2^{\bullet+}TCNQ^{\bullet-}$
			6-31G/6-31+G		
α^e_{zz}(0;0)	2.759×10^2	3.171×10^2	1.705×10^2	6.438×10^2	6.052×10^2
α^{nr}_{zz}(0;0)	5.907×10^1 *0.21*	2.561×10^1 *0.08*	4.840×10^1 *0.28*	9.416×10^1 *0.15*	8.196×10^1 *0.14*
β^e_{zzz}(0;0,0)	1.158×10^4	6.802×10^1	-1.108×10^4	3.998×10^4	2.612×10^4
β^{nr}_{zzz}(0;0,0)	2.996×10^4 *2.59*	9.406×10^3 *138*	8.393×10^3 *0.76*	3.151×10^4 *0.79*	4.529×10^3 *0.17*
γ^e_{zzzz}(0;0,0,0)	3.55×10^6	*b*	3.25×10^6	4.63×10^6	2.49×10^6
γ^{nr}_{zzzz}(0;0,0,0)	1.57×10^7 *4.42*	*b*	-1.13×10^6 *0.35*	1.87×10^7 *4.04*	6.21×10^5 *0.25*
			6-31+G/6-31+G(d)		
α^e_{zz}(0;0)	2.856×10^2	3.350×10^2	1.617×10^2	6.933×10^2	6.476×10^2
α^{nr}_{zz}(0;0)	5.282×10^1 *0.18*	3.154×10^1 *0.09*	6.493×10^1 *0.40*	1.257×10^2 *0.18*	8.416×10^1 *0.13*
β^e_{zzz}(0;0,0)	8.055×10^3	2.956×10^2	-6.421×10^3	4.623×10^4	3.002×10^4
β^{nr}_{zzz}(0;0,0)	1.106×10^4 *1.37*	8.242×10^3 *28.9*	5.721×10^3 *0.89*	5.987×10^4 *1.29*	6.173×10^3 *0.21*
γ^e_{zzzz}(0;0,0,0)	3.27×10^6	8.16×10^6	1.84×10^6	5.05×10^6	3.48×10^6
γ^{nr}_{zzzz}(0;0,0,0)	2.97×10^6 *0.91*	1.17×10^6 *0.14*	-1.03×10^6 *0.56*	4.02×10^7 *7.96*	*b*
			6-31++G(d)/6-311+G(3df)		
α^e_{zz}(0;0)	3.094×10^2	3.495×10^2	1.570×10^2	6.075×10^2	6.237×10^2
α^{nr}_{zz}(0;0)	6.944×10^1 *0.22*	4.269×10^1 *0.12*	8.685×10^1 *0.55*	1.151×10^2 *0.19*	9.776×10^1 *0.16*
β^e_{zzz}(0;0,0)	9.872×10^3	2.488×10^3	-5.148×10^3	3.008×10^4	2.205×10^4
β^{nr}_{zzz}(0;0,0)	1.874×10^4 *1.90*	1.189×10^4 *4.78*	-6.365×10^3 *1.24*	4.314×10^4 *1.43*	7.410×10^3 *0.34*
γ^e_{zzzz}(0;0,0,0)	3.40×10^6	8.94×10^6	1.38×10^6	5.17×10^6	2.18×10^6
γ^{nr}_{zzzz}(0;0,0,0)	3.26×10^6 *0.96*	-7.52×10^5 *0.08*	*b*	3.12×10^7 *6.02*	1.10×10^6 *0.50*

[a]The larger basis set is used for Li and Na, the smaller one for all other atoms. The magnitude of the ratio P^{nr}/P^e between the NR and corresponding static electronic property is given in italics. All quantities are in atomic units. [b]Finite field geometry optimizations not converged.

We checked, in addition, that the unrestricted approach used in Table 1 leads to reliable NLOP values as compared to a corresponding restricted calculation. In particular, Li@Calix, Na@Calix, and Li@$B_{10}H_{14}$ are doublets with a spin contamination of less than 0.7% and 4.2% at the UB3LYP and UMP2 levels, respectively. Whereas the spin contamination in the triplet ground state of $Li_2^{\bullet+}TCNQ^{\bullet-}$ and $Na_2^{\bullet+}TCNQ^{\bullet-}$ is negligible for UB3LYP (less than 1.0%), for UMP2 it reaches a value of approximately 42% for both molecules. In that case, however, the difference between UMP2 and ROMP2 is 0.9%, 9.0%, and 19.3% for $\overline{\alpha}^e$, β^e_{vec}, and $\gamma^e_{\|}$, respectively. On the basis of the latter results, and assuming the effect of spin contamination on the NLOP values will be smaller for cases of smaller contamination, we conclude from the results in Table 1 that UB3LYP is sufficiently reliable for the current study.

dx.doi.org/10.1021/ct300433q | J. Chem. Theory Comput. 2012, 8, 2688−2697

Table 4. Average Electronic and Nuclear Relaxation Static Linear Polarizabilities, Static First Hyperpolarizabilities, and dc-Pockels First Hyperpolarizabilities Calculated at the UB3LYP/6-31+G/6-31+G(d) Level for the Five Electride Molecules Shown in Figure 1[a]

properties	Li@Calix	Na@Calix	Li@$B_{10}H_{14}$	$Li^{\bullet+}TCNQ^{\bullet-}$	$Na_2^{\bullet+}TCNQ^{\bullet-}$
$\alpha^{e}_{xx}(0;0)$	4.296×10^2	4.775×10^2	1.416×10^2	1.506×10^2	1.738×10^2
$\alpha^{e}_{yy}(0;0)$	4.296×10^2	4.775×10^2	1.476×10^2	2.719×10^2	3.476×10^2
$\alpha^{e}_{zz}(0;0)$	2.856×10^2	3.350×10^2	1.617×10^2	6.933×10^2	6.476×10^2
$\overline{\alpha}^{e}(0;0)$	3.816×10^2	4.300×10^2	1.503×10^2	3.719×10^2	3.897×10^2
$\alpha^{nr}_{xx}(0;0)$	1.101×10^2	5.656×10^1	1.768×10^2	9.951×10^1	9.463×10^1
$\alpha^{nr}_{yy}(0;0)$	1.100×10^2	5.656×10^1	1.339×10^1	1.159×10^2	1.627×10^2
$\alpha^{nr}_{zz}(0;0)$	5.428×10^1	3.124×10^1	6.495×10^1	1.259×10^2	8.435×10^1
$\overline{\alpha}^{nr}(0;0)$	9.146×10^1 *24.0*	4.812×10^1 *11.2*	8.506×10^1 *56.6*	1.138×10^2 *30.6*	1.139×10^2 *29.2*
$\beta^{e}_{zzz}(0;0,0)$	8.055×10^3	2.956×10^2	-6.421×10^3	4.623×10^4	3.002×10^4
$\beta^{e}_{xxz}(0;0,0)$	1.193×10^3	-3.453×10^3	-4.151×10^2	-2.057×10^3	-1.288×10^3
$\beta^{e}_{yyz}(0;0,0)$	1.193×10^3	-3.453×10^3	-4.156×10^2	-7.623×10^3	-7.158×10^3
$\beta^{e}_{vec}(0;0,0)$	1.044×10^4	6.610×10^3	7.252×10^3	3.655×10^4	2.158×10^4
$\beta^{nr}_{zzz}(0;0,0)$	1.12×10^4	8.57×10^3	5.73×10^3	6.01×10^4	6.23×10^3
$\beta^{nr}_{xxz}(0;0,0)$	4.36×10^3	1.20×10^3	-3.86×10^4	3.1×10^3	-7.50×10^3
$\beta^{nr}_{yyz}(0;0,0)$	4.36×10^3	1.20×10^3	1.73×10^3	7.4×10^3	-6.23×10^3
$\beta^{nr}_{vec}(0;0,0)$	1.99×10^4 *1.91*	1.10×10^4 *1.66*	3.11×10^4 *4.29*	7.06×10^4 *1.93*	7.50×10^3 *0.35*
$\beta^{nr}_{zzz}(-\omega;\omega,0)_{\omega\to\infty}$	3.68×10^3	3.37×10^3	2.75×10^3	1.82×10^4	1.58×10^3
$\beta^{nr}_{xxz}(-\omega;\omega,0)_{\omega\to\infty}$	-1.93×10^2	-1.76×10^3	-1.51×10^1	4.45×10^3	-1.17×10^3
$\beta^{nr}_{yyz}(-\omega;\omega,0)_{\omega\to\infty}$	-1.88×10^2	-1.76×10^3	1.07×10^2	3.72×10^3	3.47×10^3
$\beta^{nr}_{vec}(-\omega;\omega,0)_{\omega\to\infty}$	7.86×10^3 *0.75*	4.29×10^3 *0.65*	2.92×10^3 *0.40*	2.35×10^4 *0.64*	2.64×10^3 *0.12*

[a]The larger basis set is used for Li and Na, and the smaller one for all other atoms. The individual components that contribute to the average values are also presented, and the magnitude of the ratio P^{nr}/P^{e} between the NR and corresponding static electronic property is given in italics. All quantities are in atomic units.

As recommended in the literature,[5a,b,d] we chose to use hybrid basis sets that combine a larger basis for describing the alkali atoms with a smaller basis set for all other atoms. In Table 2, we present a comparison between hybrid and nonhybrid basis set results for the Li@Calix molecule calculated at the UB3LYP level using UB3LYP/6-311G(d,p) optimized geometries. Quantities shown include $\overline{\alpha}^{e}(0;0)$, $\beta^{e}_{vec}(0;0,0)$, and $\gamma^{e}_{\parallel}(0;0,0,0)$, along with the unique nonzero components of the static α^{e} and β^{e} tensors as well as the diagonal components of the static γ^{e} tensor. Where only one basis set is indicated, this refers to a nonhybrid result. The rationale for a larger basis set on the alkali atom is that the electronic distribution in the electrides responsible for their large NLOP is located close to the alkali atom. Our results in Table 2 for Li@Calix support the hybrid basis set strategy. The first two basis sets provide a good example of the efficacy of this approach. Whereas the average absolute deviation in the listed 6-31G electronic NLOP values is 82% with respect to our largest basis set, this deviation is reduced to 21.5% for the 6-31G/6-31+G basis set, which adds just a single set of diffuse valence functions to the Li atom. Thus, at essentially the same computational cost, the deviation is reduced by a factor of 4. Although the overall improvement is smaller in other cases, one always gets an improvement at very low computational cost when polarization and/or ordinary valence functions on Li are added to a nonhybrid basis set. For instance, upon replacing 6-31+G by 6-31+G/6-31+G(d), the average absolute deviation decreases from 10.1% to 9.1%, and upon replacing 6-31++G(d) by 6-31++G(d)/6-311++G(d), it decreases from 8.1% to 6.9%. One hybrid basis set with very good performance is 6-31++G(d)/6-311++G(3df). It has an average absolute deviation of only 2.7%. The performance of the latter basis set is better for α and γ than for β. Taking into account the asymmetric position of the alkali atom, it is not surprising that inadequacies of the hybrid basis set affect odd-order properties, such as the first hyperpolarizability, more than even-order properties. If the reference basis set is taken to be 6-311++G(d,p) instead of 6-311++G(d,p)/6-311+G(3df), the same conclusions as above are obtained. On the basis of the results of Table 2, we have selected 6-31G/6-31+G, 6-31+G/6-31+G(d), and 6-31++G(d)/6-311++G(3df) for calculating the vibrational (hyper)polarizabilities of the set of five electrides in this study.

In Table 3, values of the diagonal component of the electronic and FF-NR contributions to the static (hyper)-polarizabilities along the symmetry axis (z) are presented. These results show that the NR contributions play an essential role in determining the static (hyper)polarizabilities. In order to discuss these contributions, we focus first on the P^{nr}/P^{e} ratios computed at our highest level, i.e., UB3LYP/6-31++G(d)/6-311++G(3df). For α_{zz}, the average P^{nr}/P^{e} for all five electrides is 0.25, with a maximum of 0.55 for Li@$B_{10}H_{14}$. The latter molecule, as noted in the Introduction, is the only one where the excess electron of the alkali atom is pulled inward. It has the smallest α^{e}_{zz} and the third largest α^{nr}_{zz}. For β_{zzz} and γ_{zzzz}, the average P^{nr}/P^{e} is 1.94 and 1.89, respectively. In the case of β_{zzz}, the largest ratio of 4.78 corresponds to Na@Calix. Again, this is due to a small electronic value (the smallest of the set) coupled with a fairly large NR contribution (again, the third largest). On the other hand, the largest γ_{zzzz} ratio is 6.02. It occurs for $Li_2^{\bullet+}TCNQ^{\bullet-}$, which also has the largest electronic second hyperpolarizability. In that case, the large P^{nr}/P^{e} is due to an extraordinary large value of $P^{nr} = 3.12 \times 10^7$ au for a medium-sized molecule. A comparison of Li@Calix with Na@Calix and $Li_2^{\bullet+}TCNQ^{\bullet-}$ with $Na_2^{\bullet+}TCNQ^{\bullet-}$ shows that, in both instances, the replacement of Li by Na leads to a reduction in all NR properties of Table 3. However, the origin of the reduction is different in the two cases. For the Li@Calix/Na@Calix pair, it is caused by a partial cancellation of different

Table 5. Average Electronic and Nuclear Relaxation Static, dc-Kerr, ESHG, and IDRI Second Hyperpolarizabilities Calculated at the B3LYP/6-31+G/6-31+G(d) Level for the Five Electride Molecules Shown in Figure 1[a]

properties	Li@Calix	Na@Calix	Li@$B_{10}H_{14}$	$Li_2^{\bullet+}TCNQ^{\bullet-}$	$Na_2^{\bullet+}TCNQ^{\bullet-}$
$\gamma^{e}_{xxxx}(0;0,0,0)$	5.58×10^6	1.00×10^7	4.14×10^5	3.86×10^5	4.61×10^5
$\gamma^{e}_{yyyy}(0;0,0,0)$	5.58×10^6	1.00×10^7	4.90×10^5	1.08×10^6	1.31×10^6
$\gamma^{e}_{zzzz}(0;0,0,0)$	3.30×10^6	8.32×10^6	1.86×10^6	5.09×10^6	3.51×10^6
$\gamma^{e}_{\parallel}(0;0,0,0)$	4.81×10^6	1.01×10^7	4.68×10^5	1.40×10^6	1.26×10^6
$\gamma^{nr}_{xxxx}(-\omega;\omega,0,0)_{\omega\to\infty}$	-9.13×10^5	5.24×10^5	-8.36×10^5	1.18×10^5	1.75×10^5
$\gamma^{nr}_{yyyy}(-\omega;\omega,0,0)_{\omega\to\infty}$	-9.13×10^5	5.24×10^5	8.63×10^3	1.10×10^5	7.51×10^5
$\gamma^{nr}_{zzzz}(-\omega;\omega,0,0)_{\omega\to\infty}$	1.24×10^6	-6.02×10^5	-1.05×10^6	1.13×10^7	5.58×10^5
$\gamma^{nr}_{\parallel}(-\omega;\omega,0,0)_{\omega\to\infty}$	-3.09×10^5 *0.06*	1.20×10^5 *0.01*	-7.56×10^5 *1.62*	2.75×10^6 *1.97*	5.51×10^5 *0.44*
$\gamma^{nr}_{xxxx}(-2\omega;\omega,\omega,0)_{\omega\to\infty}$	-9.43×10^5	-8.48×10^5	-3.85×10^4	-1.66×10^5	-1.16×10^3
$\gamma^{nr}_{yyyy}(-2\omega;\omega,\omega,0)_{\omega\to\infty}$	-9.42×10^5	-8.48×10^5	-1.76×10^3	-4.58×10^5	-9.89×10^5
$\gamma^{nr}_{zzzz}(-2\omega;\omega,\omega,0)_{\omega\to\infty}$	3.07×10^5	-5.97×10^5	-7.19×10^5	1.30×10^6	-3.06×10^5
$\gamma^{nr}_{\parallel}(-2\omega;\omega,\omega,0)_{\omega\to\infty}$	-6.71×10^5 *0.14*	-7.40×10^5 *0.07*	-1.81×10^5 *0.39*	1.44×10^5 *0.10*	-2.52×10^5 *0.20*
$\gamma^{nr}_{xxxx}(-\omega;\omega,-\omega,\omega)_{\omega\to\infty}$	3.33×10^6	4.58×10^6	1.25×10^4	1.05×10^5	1.29×10^5
$\gamma^{nr}_{yyyy}(-\omega;\omega,-\omega,\omega)_{\omega\to\infty}$	3.33×10^6	4.58×10^6	1.91×10^4	1.33×10^6	3.21×10^6
$\gamma^{nr}_{zzzz}(-\omega;\omega,-\omega,\omega)_{\omega\to\infty}$	8.18×10^5	1.16×10^6	4.23×10^5	1.34×10^7	2.72×10^6
$\gamma^{nr}_{\parallel}(-\omega;\omega,-\omega,\omega)_{\omega\to\infty}$	2.62×10^6 *0.54*	3.18×10^6 *0.32*	1.05×10^5 *0.22*	3.49×10^6 *2.50*	1.69×10^6 *1.34*

[a]The larger basis set is used for Li and Na and the smaller one for all other atoms. The diagonal components are also presented, and the magnitude of the absolute value of the ratio P^{nr}/P^{e} between the NR and corresponding static electronic property is given in italics. All quantities are in atomic units.

BKPT terms in the Na@Calix molecule. On the other hand, for the $Li_2^{\bullet+}TCNQ^{\bullet-}/Na_2^{\bullet+}TCNQ^{\bullet-}$ pair, it is due to a strong decrease in the $Na_2^{\bullet+}TCNQ^{\bullet-}$ BKPT terms that contain α derivatives.

The NR contributions to the NLOP for our set of electrides show slower convergence with respect to the size of the basis set than the electronic contributions. For the smallest $\beta^{nr}_{zzz}(0;0,0)$ and $\gamma^{nr}_{zzzz}(0;0,0,0)$ values (obtained with the 6-31++G(d)/6-311+G(3df) basis set), the 6-31+G/6-31+G(d) basis set does not even give the correct sign. Nevertheless, the average absolute deviation in the diagonal z component of the total property value (i.e., electronic + nuclear relaxation contributions) calculated using the 6-31+G/6-31+G(d) basis, as compared to the largest basis, is only 8% and 15% for α and γ, respectively. It is less good, however, for β, in which case the average absolute deviation is 47%. Thus, the 6-31+G/6-31+G(d) basis set leads to semiquantitative accuracy for linear polarizabilities and second hyperpolarizabilites but can only be used for qualitative conclusions as far as the first hyperpolarizability is concerned. Despite this last mentioned difficulty, we used the 6-31+G/6-31+G(d) basis set going forward since the set of NR calculations for all the remaining components of the static and dynamic (hyper)polarizability tensors with the largest basis set would have been too demanding.

In Tables 4 and 5, our results are shown for $\overline{\alpha}^{e}(0;0)$, $\overline{\alpha}^{nr}(0;0)$, $\beta^{e}_{vec}(0;0,0)$, $\beta^{nr}_{vec}(0;0,0)$, $\beta^{nr}_{vec}(-\omega;\omega,0)_{\omega\to\infty}$, $\gamma^{e}_{\parallel}(0;0,0,0)$, $\gamma^{nr}_{\parallel}(-\omega;\omega,0,0)_{\omega\to\infty}$, $\gamma^{nr}_{\parallel}(-2\omega;\omega,\omega,0)_{\omega\to\infty}$, and $\gamma^{nr}_{\parallel}(-\omega;\omega,-\omega,\omega)_{\omega\to\infty}$. We also present the diagonal components of the α and γ tensors (both electronic and NR contributions), as well as the three components of the β tensor that have the largest value. All components of the (hyper)-polarizability tensors were computed using only the three first-order FICs (χ^{x}_{1}, χ^{y}_{1}, χ^{z}_{1}) and the six harmonic second order FICs ($\chi^{xx}_{2,har}$, $\chi^{xy}_{2,har}$, $\chi^{yy}_{2,har}$, $\chi^{xz}_{2,har}$, $\chi^{yz}_{2,har}$, $\chi^{zz}_{2,har}$). As explained in the previous section, only one or two of these FICs would be required if we were interested in just a single component of any NR (hyper)polarizability tensor. As noted earlier, FICs were not employed to obtain $\gamma^{nr}_{\parallel}(0;0,0,0)$ because the required anharmonic second-order FICs are computationally too expensive to determine.

We now analyze, again, the ratio P^{nr}/P^{e} for the static linear polarizability and first hyperpolarizabilty, but this time for the average tensor values (see later for the average static second hyperpolarizability). In fact, our conclusions are very similar to those obtained for the diagonal z component given in Table 3. The average (maximum) ratios for $\overline{\alpha}(0;0)$ and $\beta_{vec}(0;0,0)$ are 0.30 (0.57) and 2.03 (4.29), respectively. For both properties, the maximum pertains to Li@$B_{10}H_{14}$. From these results, we conclude that the NR contribution is necessary in order to obtain an accurate value of the average static linear polarizability and essential for a reliable value of the static β_{vec}.

Next, we turn to the NR dynamic properties. Equations 7, 9−11 have fewer terms on the right-hand side than appear in the corresponding static property relation. This occurs because some, or all, of the anharmonic terms vanish in the IOF approximation. The IOF approximation also causes the coefficient of each remaining NR dynamic term to be reduced from that of the corresponding static term. For instance, the diagonal component of the NR dc-Pockels β is 1/3 the corresponding (double harmonic) static β, i.e. $[\mu\alpha]^{0}_{1zzz} = 1/3\,[\mu\alpha]^{0}_{2zzz}$ (see ref 11d for more details). Thus, the magnitude of an NR dynamic property will generally be smaller than that of the corresponding static property, although there may be exceptions due to higher-order static contributions of opposite sign. Moreover, as a rough general proposition, the NR (hyper)polarizability of a given molecule will increase the larger the number of static external fields.

From Tables 4 and 5, we see that the averages (maxima) of P^{nr}/P^{e} for the dc-Pockels effect ($\beta^{nr}_{vec}(-\omega;\omega,0)_{\omega\to\infty}$), dc-Kerr effect ($\gamma^{nr}_{\parallel}(-\omega;\omega,0,0)_{\omega\to\infty}$), EFISH ($\gamma^{nr}_{\parallel}(-2\omega;\omega,\omega,0)_{\omega\to\infty}$), and IDRI ($\gamma^{nr}_{\parallel}(-\omega;\omega,-\omega,\omega)_{\omega\to\infty}$) are 0.51 (0.75), 0.82 (1.97), 0.18 (0.39), and 0.99 (2.50), respectively. At the same level of treatment, the average value of P^{nr}/P^{e} for γ^{nr}_{zzzz} (0;0,0,0) is 2.39. These results reflect the general behavior described in the previous paragraph, with the unique exception of IDRI. IDRI is exceptional because of a cancellation between the $+\omega$ and $-\omega$ optical frequencies. As a result, it behaves like a property

Table 6. Average Electronic and Nuclear Relaxation Static Linear Polarizabilities, Static First Hyperpolarizabilities, and dc-Pockels First Hyperpolarizabilities Calculated at the UB3LYP/6-31+G/6-31+G(d) Level for the Calix and TCNQ Ligands (see Figure 2), the Negatively Charged $TCNQ^{\bullet-}$, and the Positively Charged $[Li@Calix]^+$ and $[Li_2\text{-}TCNQ]^+$[a]

properties	Calix	$[Li@Calix]^+$	TCNQ	$TCNQ^{\bullet-}$	$[Li_2TCNQ]^+$
$\alpha^{e}_{xx}(0;0)$	2.491×10^2	2.674×10^2	7.195×10^1	8.123×10^1	7.757×10^1
$\alpha^{e}_{yy}(0;0)$	2.491×10^2	2.674×10^2	1.717×10^2	1.961×10^2	2.157×10^2
$\alpha^{e}_{zz}(0;0)$	2.352×10^2	1.918×10^2	4.241×10^2	5.104×10^2	3.376×10^2
$\bar{\alpha}^{e}(0;0)$	2.445×10^2	2.422×10^2	2.226×10^2	2.626×10^2	2.103×10^2
$\alpha^{nr}_{xx}(0;0)$	5.571×10^1	3.097×10^2	1.237×10^2	1.032×10^2	5.451×10^2
$\alpha^{nr}_{yy}(0;0)$	5.571×10^1	3.097×10^2	2.054×10^1	1.624×10^1	8.458×10^1
$\alpha^{nr}_{zz}(0;0)$	1.787×10^1	1.964×10^1	1.427×10^1	2.379×10^1	4.586×10^2
$\bar{\alpha}^{nr}(0;0)$	4.310×10^1 *0.18*	2.130×10^2 *0.88*	5.284×10^1 *0.24*	4.776×10^1 *0.18*	3.628×10^2 *1.72*
$\beta^{e}_{zzz}(0;0,0)$	0.000	-7.442×10^1	0.000	0.000	1.022×10^4
$\beta^{e}_{xxz}(0;0,0)$	-2.567×10^2	-1.320×10^2	0.000	0.000	-1.882×10^2
$\beta^{e}_{yyz}(0;0,0)$	2.567×10^2	-1.320×10^2	0.000	0.000	-1.627×10^3
$\beta^{e}_{vec}(0;0,0)$	0.000	3.383×10^2	0.000	0.000	8.402×10^3
$\beta^{nr}_{zzz}(0;0,0)$	0.00	7.23×10^2	0.00	0.00	-3.65×10^4
$\beta^{nr}_{xxz}(0;0,0)$	-1.50×10^3	-4.99×10^3	0.00	0.00	-3.49×10^4
$\beta^{nr}_{yyz}(0;0,0)$	1.50×10^0	-4.99×10^3	0.00	0.00	1.38×10^4
$\beta^{nr}_{vec}(0;0,0)$	0.00	9.26×10^3 *27.36*	0.00	0.00	5.77×10^4 *6.86*
$\beta^{nr}_{zzz}(-\omega;\omega,0)_{\omega\to\infty}$	0.00	2.57×10^2	0.00	0.00	3.97×10^3
$\beta^{nr}_{xxz}(-\omega;\omega,0)_{\omega\to\infty}$	-7.15×10^2	-4.16×10^1	0.00	0.00	-8.44×10^2
$\beta^{nr}_{yyz}(-\omega;\omega,0)_{\omega\to\infty}$	7.15×10^2	-4.16×10^1	0.00	0.00	$-7.75E \times 10^2$
$\beta^{nr}_{vec}(-\omega;\omega,0)_{\omega\to\infty}$	0.00	6.70×10^1 *0.20*	0.00	0.00	2.36×10^3 *0.28*

[a]The larger basis set is used for Li and Na, and the smaller one for all other atoms. The individual components that contribute to the average values are also presented, and the magnitude of the ratio P^{nr}/P^{e} between the NR and corresponding static electronic property is given in italics. All quantities are in atomic units.

described by two static external fields. Indeed, due to the IOF approximation only eight of the 24 terms (that arise from permutation of indices) are eliminated from the formula for the nuclear relaxation contribution to the static γ so that $[\alpha^2]^0_{2'zzzz} = 2/3\ [\alpha^2]^0_{3zzzz}$ (see ref 11d for more details). It is clear from the numerical values cited at the beginning of this paragraph that it is essential to include the NR contribution to obtain a meaningful value of the IDRI. The same is true of the dc-Pockels and dc-Kerr effects and, to a somewhat lesser extent, EFISH as well.

The importance of anharmonicity is variable for this set of electrides. In the case of $Li_2^{\bullet+}TCNQ^{\bullet-}$, the double harmonic terms are clearly dominant for the NR first hyperpolarizability. This can be deduced from the value of $\beta^{nr}_{vec}(-\omega;\omega,0)_{\omega\to\infty}$, which is very close to one-third the value of $\beta^{nr}_{vec}(0;0,0)$, as it would be if anharmonicity were entirely negligible. The same is true for the NR contributions to the first hyperpolarizability of Li@Calix and Na@Calix but not the other two electrides.

The harmonic FICs used in this paper do not allow us to obtain an accurate $\gamma^{nr}_{\parallel}(0;0,0,0)$, although they do allow a rough value to be estimated. In fact, the sole term that it is not completely determined by the harmonic FICs is $[\mu^4]^{II}$. For $Li_2^{\bullet+}TCNQ^{\bullet-}$, we can surmise that this term is negligible. One piece of evidence is the fact that the value of $\gamma^{nr}_{zzzz}(0;0,0,0)$ obtained using only harmonic FICs agrees very well (error smaller than 2%) with the "exact" FF-NR value. This does not occur, in our experience, if $[\mu^4]^{II}$ is significant (see one example below). A second piece of evidence is that the approximate $[\mu^4]^{II}$ computed with the harmonic FICs (see ref 14c for method of calculation) is very small. As far as $Li_2^{\bullet+}TCNQ^{\bullet-}$ is concerned, then, the two largest terms in the expression for the static γ^{nr} in eq 8 are $[\alpha^2]^0$ and $[\mu^2\alpha]^I$. These terms lead to P^{nr}/P^{e} values of 1.97 and 2.50 for $\gamma^{nr}_{\parallel}(-\omega;\omega,0,0)_{\omega\to\infty}$ and $\gamma^{nr}_{\parallel}(-\omega;\omega,-\omega,\omega)_{\omega\to\infty}$, respectively. On the other hand, $[\mu\beta]^0$ and $[\mu^4]^{II}$ are, at least, 1 order of magnitude smaller. Note that the first of these two square bracket terms is responsible for the small value of $\gamma^{nr}_{\parallel}(-2\omega;\omega,\omega,0)_{\omega\to\infty}$ (*cf.* eq 10). For $Li_2^{\bullet+}TCNQ^{\bullet-}$, the largest terms in both the static β^{nr}_{vec} and the static $\gamma^{nr}_{\parallel}$ are those that involve first derivatives of the linear polarizability (with respect to nuclear coordinates, which occur in $[\mu\alpha]^0$, $[\alpha^2]^0$, and $[\mu^2\alpha]^I$).

As opposed to $Li_2^{\bullet+}TCNQ^{\bullet-}$, anharmonicity plays a dominant role in the NR contributions to the average static first and second hyperpolarizability of $Li@B_{10}H_{14}$. In the expression for the static β^{nr} given by eq 2 $[\mu^3]^I$ is the largest term for this molecule. Consequently, the P^{nr}/P^{e} ratio of 4.29 for $\beta^{nr}_{vec}(0;0,0)$ is 1 order of magnitude larger than the corresponding ratio for $\beta^{nr}_{vec}(-\omega;\omega,0)_{\omega\to\infty}$. For the NR static second hyperpolarizability obtained using only harmonic FICs, the largest term in eq 8 is the approximate $[\mu^4]^{II}$. For $Li@B_{10}H_{14}$, this approximation leads to a value of $\gamma^{nr}_{zzzz}(0;0,0,0)$ which is in error by 78% with respect to the "exact" value obtained through the FF-NR approach. Thus, the approximate average values of $[\mu^4]^{II}$ and $\gamma^{nr}_{\parallel}(0;0,0,0)$ should be taken with caution. Nonetheless, it is interesting that the approximate $\gamma^{nr}_{\parallel}(0;0,0,0)$ leads to a huge P^{nr}/P^{e} of 64.12. The next largest term after (the approximate) $[\mu^4]^{II}$, although 1 order of magnitude smaller, is $[\mu^2\alpha]^I$. The latter leads to a P^{nr}/P^{e} value of 1.62 for $\gamma^{nr}_{\parallel}(-\omega;\omega,0,0)_{\omega\to\infty}$ (ESHG is the only dynamic process that depends on anharmonicity in the NR treatment). Finally, for this molecule, $[\alpha^2]^0$ is the smallest contributor to the static γ^{nr}. Hence, the P^{nr}/P^{e} value for IDRI is only 0.22, which is the smallest ratio for all the dynamic second hyperpolarizabilities. The magnitude of the various NR terms for $Li@B_{10}H_{14}$ is determined by the dipole derivatives; the higher the power of μ in the square bracket representation, the larger will be the contribution of that term. In the case of $\gamma^{nr}_{\parallel}(0;0,0,0)$, for example, the order from the largest to the

Table 7. Average Electronic and Nuclear Relaxation Static, dc-Kerr, ESHG, and IDRI Second Hyperpolarizabilities Calculated at the UB3LYP/6-31+G/6-31+G(d) Level for the Calix and TCNQ Ligands (see Figure 2), the Negatively Charged $TCNQ^{\bullet -}$, and the Positively Charged $[Li@Calix]^+$ and $[Li_2\text{-}TCNQ]^+$[a]

properties	Calix	$[Li@Calix]^+$	TCNQ	$TCNQ^{\bullet -}$	$[Li_2\text{-}TCNQ]^+$
$\gamma^{e}_{xxxx}(0;0,0,0)$	1.16×10^5	1.20×10^5	1.42×10^4	2.32×10^4	2.16×10^4
$\gamma^{e}_{yyyy}(0;0,0,0)$	1.16×10^5	1.20×10^5	3.29×10^4	3.77×10^4	1.53×10^5
$\gamma^{e}_{zzzz}(0;0,0,0)$	5.67×10^4	3.29×10^4	-1.96×10^4	-2.94×10^6	1.57×10^6
$\gamma^{e}_{\parallel}(0;0,0,0)$	9.55×10^4	8.40×10^4	4.82×10^4	-5.16×10^5	4.21×10^5
$\gamma^{nr}_{xxxx}(-\omega;\omega,0,0)_{\omega\to\infty}$	6.44×10^4	-1.38×10^5	1.70×10^5	1.02×10^5	2.57×10^5
$\gamma^{nr}_{yyyy}(-\omega;\omega,0,0)_{\omega\to\infty}$	6.44×10^4	-1.38×10^5	-5.69×10^3	3.84×10^3	-7.82×10^4
$\gamma^{nr}_{zzzz}(-\omega;\omega,0,0)_{\omega\to\infty}$	-3.00×10^3	1.97×10^4	2.53×10^5	5.86×10^5	-1.57×10^5
$\gamma^{nr}_{\parallel}(-\omega;\omega,0,0)_{\omega\to\infty}$	4.51×10^4 *0.47*	-8.72×10^4 *1.04*	5.67×10^4 *1.18*	1.22×10^5 *0.24*	-3.53×10^4 *0.08*
$\gamma^{nr}_{xxxx}(-2\omega;\omega,\omega,0)_{\omega\to\infty}$	4.42×10^3	-8.04×10^4	-1.09×10^4	-1.16×10^4	-2.85×10^4
$\gamma^{nr}_{yyyy}(-2\omega;\omega,\omega,0)_{\omega\to\infty}$	4.42×10^3	-8.04×10^4	-5.62×10^2	2.62×10^3	-1.68×10^4
$\gamma^{nr}_{zzzz}(-2\omega;\omega,\omega,0)_{\omega\to\infty}$	-1.21×10^3	-3.00×10^2	1.87×10^3	1.50×10^4	-1.34×10^5
$\gamma^{nr}_{\parallel}(-2\omega;\omega,\omega,0)_{\omega\to\infty}$	1.12×10^3 *0.01*	-5.18×10^4 *0.62*	-5.61×10^3 *0.12*	-5.94×10^3 *0.01*	-8.39×10^4 *0.20*
$\gamma^{nr}_{xxxx}(-\omega;\omega,-\omega,\omega)_{\omega\to\infty}$	1.12×10^5	1.81×10^5	3.52×10^2	4.49×10^2	3.85×10^2
$\gamma^{nr}_{yyyy}(-\omega;\omega,-\omega,\omega)_{\omega\to\infty}$	1.12×10^5	1.81×10^5	2.53×10^4	2.81×10^4	3.54×10^4
$\gamma^{nr}_{zzzz}(-\omega;\omega,-\omega,\omega)_{\omega\to\infty}$	5.65×10^4	4.03×10^4	5.28×10^5	1.17×10^6	2.52×10^5
$\gamma^{nr}_{\parallel}(-\omega;\omega,-\omega,\omega)_{\omega\to\infty}$	7.77×10^4 *0.81*	7.80×10^4 *0.93*	1.26×10^5 *2.61*	2.62×10^5 *0.51*	8.29×10^4 *0.20*

[a]The larger basis set is used for Li and Na and the smaller basis set for all other atoms. The diagonal components are also presented, and the magnitude of the absolute value of the ratio P^{nr}/P^{e} between the NR and corresponding static electronic property is given in italics. All quantities are in atomic units.

smallest is $[\mu^4]^{II}$, $[\mu^2\alpha]^{I}$, $[\mu\beta]^0$, and $[\alpha^2]^0$. The relative weight of the anharmonicity contribution to the NR hyperpolarizabilities of the remaining three molecules falls in between the two extreme cases discussed above. It is higher than for $Li_2^{\bullet+}TCNQ^{\bullet-}$ but lower than for $Li@B_{10}H_{14}$. Nevertheless, anharmonicity is also dominant in the case of $Na_2^{\bullet+}TCNQ^{\bullet-}$.

The diagonal component along the z symmetry axis is dominant for both the electronic and NR contributions to $\beta^{nr}_{vec}(0;0,0)$ in all five electrides. For the average linear polarizability, there is not a single dominant component. On the other hand, for $\gamma_{\parallel}$, the diagonal z component makes the dominant contribution to both the electronic and NR term in $Li@B_{10}H_{14}$ and $Li_2^{\bullet+}TCNQ^{\bullet-}$, but not the other electrides.

The nine FICs (three first-order and six second-order), computed at the B3LYP/6-31+G/6-31+G(d) level for each of the five electrides studied in this work, are shown in the Supporting Information. For Li@Calix, Na@Calix, and $Li@B_{10}H_{14}$, the first-order FIC χ^{z}_{1}, which yields the dominant contribution to $\beta^{nr}_{vec}(0;0,0)$, involves almost entirely a motion of the alkali atom along the z symmetry axis. However, this is not the case for χ^{z}_{1} of the two TCNQ adducts. For the latter, the four nitrogen atoms also undergo a significant displacement. The other two (perpendicular) components of the first-order FIC are also dominated by alkali atom displacements in Li@Calix and $Li@B_{10}H_{14}$ (but not in Na@Calix). Hence, for these two electrides, all of the vibrational NLO properties that depend only on first order FICs (i.e., $\alpha^{nr}(0;0)$, $\beta^{nr}(0;0,0)$, $\beta^{nr}(-\omega;\omega,0)_{\omega\to\infty}$, and $\gamma^{nr}(-2\omega;\omega,\omega,0)_{\omega\to\infty}$) could be computed with a reduced-dimensionality approach that considers only the movement of the Li atoms. On the other hand, for the Na-containing electrides, the displacement of the alkali atom(s) makes a minor (or negligible) contribution to the perpendicular first-order FICs.

As opposed to the first-order FICs, the motion of alkali atoms does not play a major role, for the most part, in the harmonic second-order FICs of Li@Calix, Na@Calix, and $Li@B_{10}H_{14}$. The only exceptions are $\chi^{xz}_{2,har}$ and $\chi^{yz}_{2,har}$ of Na@Calix and $\chi^{yy}_{2,har}$ of $Li@B_{10}H_{14}$. On the contrary, for $Li_2^{\bullet+}TCNQ^{\bullet-}$ and $Na_2^{\bullet+}TCNQ^{\bullet-}$, the alkali atom displacements are more important. This is especially true for $\chi^{xx}_{2,har}$ and $\chi^{xy}_{2,har}$ of $Li_2^{\bullet+}TCNQ^{\bullet-}$ and $\chi^{xx}_{2,har}$ of $Na_2^{\bullet+}TCNQ^{\bullet-}$. The alkali atoms also play a significant role in all of the other harmonic second-order FICs of these two electrides with the only exceptions being $\chi^{yy}_{2,har}$ and $\chi^{xz}_{2,har}$ of $Na_2^{\bullet+}TCNQ^{\bullet-}$.

Gu and co-workers have shown that, when either Li or an electron is removed from Li@Calix, $\beta^{e}_{vec}(0;0,0)$ is reduced by more than 1 order of magnitude.[5a] They also showed that removal of the two Li atoms from $Li_2^{\bullet+}TCNQ^{\bullet-}$ leads to a similar reduction in $\gamma^{e}_{\parallel}(0;0,0,0)$.[5b] Here, in order to evaluate the role of the loosely bound electron, we present (see Tables 6 and 7) both the electronic and NR contributions for (1) the neutral calix and TCNQ ligands, (2) the positively charged $[Li@Calix]^+$ and $[Li_2TCNQ]^+$ molecules, and (3) the negatively charged $TCNQ^{\bullet-}$ ligand. For the charged species, the origin is chosen as the center of mass. With this choice, as opposed to an origin at the center of nuclear charge (for example), the dipole moment operator is independent of the normal coordinate displacements. Hence, the vibrational (hyper)polarizabilities are not affected directly by the molecular charge (although, of course, there is an indirect effect due to the change in electronic structure). In order to calculate the NR contributions, the molecules must be in their equilibrium geometry. So we have reoptimized the geometries at the B3LYP/6-31+G/6-31+G(d) level, choosing always the global minimum. An important conformational change occurs in the case of the neutral Calix ligand. This ligand takes the 1,3-alternate conformation, in contrast with Li@Calix and $[Li@Calix]^+$, which both have the cone conformation (see Figures 1 and 2). Nevertheless, as we discuss below, the drastic reduction in NLO properties found when Li is removed from Li@Calix is not due to the change in ligand conformation but rather to the loss of electride character.

By symmetry, $\beta_{vec}(0;0,0)$ vanishes for the neutral calix and TCNQ ligands. However, the average static linear polarizability and second hyperpolarizability show a major reduction, in comparison with the corresponding electride properties, for

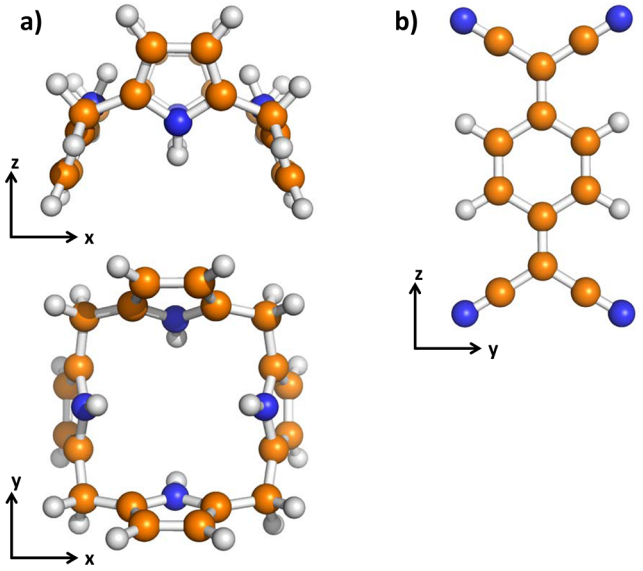

Figure 2. B3LYP/6-31+G/6-31+G(d) optimized geometries of (a) Calix and (b) TCNQ ligands.

both the electronic and NR contributions. For $\bar{\alpha}$, both contributions are reduced to about half the electride value. For $\gamma_{\|}$, the reduction is far stronger since the ligand value is only (on average) about 4% that of the electride. If an electron is added to the neutral TCNQ ligand, the NR contributions increase only slightly. On the other hand, as expected, the electronic values strongly increase although $\bar{\alpha}^{e}$ and $\gamma_{\|}^{e}$ remain smaller than those of the corresponding neutral electride. Thus, the huge electronic and vibrational NLO properties of the electrides are not only the fruit of the diffuse excess electron distribution but also arise from the fact that this distribution is not centered on any of the atoms.

Finally, for the positively charged $[Li@Calix]^+$ and $[Li_2TCNQ]^+$ molecules, we have a more complex scenario. Comparison with their electride counterparts shows that the average electronic linear polarizability is cut in half. However, the nuclear relaxation contributions to $\bar{\alpha}^{nr}$, somewhat surprisingly, increase by a factor of 2.3 and 3.1 for $[Li@Calix]^+$ and $[Li_2TCNQ]^+$, respectively. The reason for this increase is the fact that the two cations have larger dipole moment derivatives than their neutral electride counterparts. For the average electronic hyperpolarizabilities, the decrease in the case of $[Li@Calix]^+$ is close to 2 orders of magnitude, whereas in the case of $[Li_2TCNQ]^+$, the ratios of β_{vec}^{e} and $\gamma_{\|}^{e}$ with respect to their electride counterparts are 0.23 and 0.30, respectively. The smaller reductions for the latter molecule are probably associated with partial retention of electride character due to the second alkali atom in $[Li_2TCNQ]^+$.

For the average NR hyperpolarizabilities, the change with respect to the corresponding electride also depends strongly on the property. The average (maximum) magnitude of the ratio for both properties, with respect to the corresponding electride, is 0.17 (0.47) for $[Li@Calix]^+$ and 0.30 (0.82) for $[Li_2TCNQ]^+$. Although the decrease is less for $[Li_2TCNQ]^+$ than for $[Li@Calix]^+$, the difference between the two is not as large as for the electronic contribution.

4. SUMMARY AND CONCLUSIONS

It is well-known that electrides have very large NLO electronic properties. The main goal of this study has been to determine and analyze the vibrational, as compared to the electronic, NLO properties for a representative set of electrides: Li@Calix, Na@Calix, $Li@B_{10}H_{14}$, $Li_2^{\bullet+}TCNQ^{\bullet-}$, and $Na_2^{\bullet+}TCNQ^{\bullet-}$. Our values were obtained by applying the UB3LYP method with a tailored hybrid basis set. Both the method and basis set were carefully checked as to their reliability. Nevertheless, due to their special electronic structure, the electrides deserve further study regarding the effect of different DFT functionals on the electronic and vibrational NLO properties. We plan to investigate this point in the future.

Vibrational NLO properties were calculated by the nuclear relaxation (NR) method using field-induced coordinates (FICs) and the infinite optical frequency (IOF) approximation for dynamic processes. The results vary depending upon the electride and the NLO process. In general, however, we find that the static β_{vec} and $\gamma_{\|}$ exceed the corresponding electronic property values, sometimes in the latter case by more than an order of magnitude. As far as dynamic properties are concerned, the largest NR vibrational effects occur for IDRI and the dc-Kerr effect. On average, they are roughly the same as the corresponding static electronic hyperpolarizability; in particular cases, they may be twice as large or more. Although the relative NR contribution for the dc-Pockels effect and EFISH is smaller, this contribution is certainly significant. The same may be said of the average linear polarizability.

Substitution of Li for Na leads to reduced NR property values but for different reasons in the two cases studied. Although motion of the alkali atom(s) along the symmetry axis is often the primary source of the NR vibrational properties, particularly for β, that is not always the case. The role of anharmonicity in the (NR) hyperpolarizabilities is variable. It plays a dominant role for the first and second hyperpolarizability of $Li@B_{10}H_{14}$ but is negligible for the first (though not the second) hyperpolarizability of $Li_2^{\bullet+}TCNQ^{\bullet-}$. This means that higher order anharmonicity corrections may be important (see ref 9b) for the borane adduct.

For the neutral and negatively charged adducts, the NR contributions decrease by more than 1 order of magnitude with respect to the corresponding electride properties. When one electron is removed from the electrides, the reduction in the NR hyperpolarizabilites is smaller but still significant (an average reduction by a factor of 4). Our analysis shows that the NR vibrational nonlinear optical properties of the electrides are a result of both the diffuse electron distribution and the location of the excess electron density at a site different from any of the atoms.

■ ASSOCIATED CONTENT

Supporting Information

Figures showing the nine FICs (three first-order; six second-order), computed at the B3LYP/6-31+G/6-31+G(d) level, that were used for each of the five electrides studied in this work. Geometries evaluated at the B3LYP/6-31++G(d)/6-311++G(3df) level are also given. This information is available free of charge via the Internet at http://pubs.acs.org/.

■ AUTHOR INFORMATION

Corresponding Author

*Phone: +34 972418272. Fax: +34 972418356. E-mail: josepm.luis@udg.edu.

Notes

The authors declare no competing financial interest.

■ ACKNOWLEDGMENTS

The following organizations are thanked for financial support: the Spanish Ministerio de Ciencia e Innovación (MICINN, CTQ2011-23156/BQU) and the DIUE of the Generalitat de Catalunya (2009SGR637). M.G.-B. thanks the Spanish MEC for a doctoral fellowship, no. AP2010-2517. Support for the research of M.S. was received through the ICREA Academia 2009 prize for excellence in research funded by the DIUE of the Generalitat de Catalunya. Financial support from MICINN and the FEDER fund (European Fund for Regional Development) was provided by grant UNGI08-4E-003.

■ REFERENCES

(1) (a) Dye, J. L. *Science* **2003**, *301*, 607−608. (b) Matsuishi, S.; Toda, Y.; Miyakawa, M.; Hayashi, K.; Kamiya, T.; Hirano, M.; Tanaka, I.; Hosono, H. *Science* **2003**, *301*, 626−629. (c) Kim, S. W.; Shimoyama, T.; Hosono, H. *Science* **2011**, *333*, 71−74. (d) Redko, M. Y.; Jackson, J. E.; Huang, R. H.; Dye, J. L. *J. Am. Chem. Soc.* **2005**, *127*, 12416−12422. (e) Dye, J. L. *Acc. Chem. Res.* **2009**, *42*, 1564−1572.

(2) (a) Dye, J. L. *Prog. Inorg. Chem.* **1984**, *32*, 327−441. (b) Dye, J. L. *Inorg. Chem.* **1997**, *36*, 3816−3826.

(3) (a) Barrer, R. M.; Cole, J. F. *J. Phys. Chem. Solids* **1968**, *29*, 1755−1758. (b) Srdanov, V. I.; Stucky, G. D.; Lippmaa, E.; Engelhardt, G. *Phys. Rev. Lett.* **1998**, *80*, 2449−2452.

(4) Palacios, L.; De La Torre, A. G.; Bruque, S.; García-Munoz, J. L.; García-Granda, S.; Sheptyakov, D.; Aranda, M. A. G. *Inorg. Chem.* **2007**, *46*, 4167−4176.

(5) (a) Chen, W.; Li, Z. R.; Wu, D.; Li, Y.; Sun, C. C.; Gu, F. L. *J. Am. Chem. Soc.* **2005**, *127*, 10977−10981. (b) Li, Z. J.; Wang, F. F.; Li, Z. R.; Xu, H. L.; Huang, X. R.; Wu, D.; Chen, W.; Yu, G. T.; Gu, F. L.; Aoki, Y. *Phys. Chem. Chem. Phys.* **2009**, *11*, 402−408. (c) Muhammad, S.; Xu, H. L.; Liao, Y.; Kan, Y. H.; Su, Z. M. *J. Am. Chem. Soc.* **2009**, *131*, 11833−11840. (d) Ma, F.; Li, Z. R.; Xu, H. L.; Li, Z. J.; Li, Z. S.; Aoki, Y.; Gu, F. L. *J. Phys. Chem. A* **2008**, *112*, 11462−11467.

(6) (a) Prasad, P. N.; Williams, D. J. *Introduction to Nonlinear Optical Effects in Molecules and Polymers*; Wiley: New York, 1990; pp 272−294. (b) Asselberghs, I.; Hennrich, G.; McCleverty, J.; Boubekeur-Lecaque, L.; Coe, B. J.; Clays, K. Organic materials for molecular switching. In *Organic Optoelectronics and Photonics III*; Heremans, P. L., Muccini, M., Meulenkamp, E. A., Eds.; Spie-int Soc Optical Engineering: Strasbourg, France, 2008; pp 69991W-1−8.

(7) Bishop, D. M.; Kirtman, B.; Champagne, B. *J. Chem. Phys.* **1997**, *107*, 5780−5787.

(8) Bishop, D. M.; Norman, P. In *Handbook of Advanced Electronic and Photonic Materials*; Nalwas, H. S., Ed.; Academic: San Diego, CA, 2001; Vol. *9*, pp 1−240.

(9) (a) Loboda, O.; Zalesny, R.; Avramopoulos, A.; Luis, J. M.; Kirtman, B.; Tagmatarchis, N.; Reis, H.; Papadopoulos, M. G. *J. Phys. Chem. A* **2009**, *113*, 1159−1170. (b) Luis, J. M.; Reis, H.; Papadopoulos, M.; Kirtman, B. *J. Chem. Phys.* **2009**, *131*, 034116. (c) Dutra, A. S.; Castro, M. A.; Fonseca, T. L.; Fileti, E. E.; Canuto, S. *J. Chem. Phys.* **2010**, *132*, 034307. (d) Zalesny, R.; Bulik, I. W.; Bartkowiak, W.; Luis, J. M.; Avramopoulos, A.; Papadopoulos, M. G.; Krawczyk, P. *J. Chem. Phys.* **2010**, *133*, 244308. (e) Ferrabone, M.; Kirtman, B.; Rerat, M.; Orlando, R.; Dovesi, R. *Phys. Rev. B* **2011**, 83. (f) Labidi, N. S.; Djebaili, A.; Rouina, I. *J. Saudi Chem. Soc.* **2011**, *15*, 29−37. (g) Naves, E. S.; Castro, M. A.; Fonseca, T. L. *J. Chem. Phys.* **2011**, *134*, 054315. (h) Reis, H.; Loboda, O.; Avramopoulos, A.; Papadopoulos, M. G.; Kirtman, B.; Luis, J. M.; Zalesny, R. *J. Comput. Chem.* **2011**, *32*, 908−914. (i) Skwara, B.; Gora, R. W.; Zalesny, R.; Lipkowski, P.; Bartkowiak, W.; Reis, H.; Papadopoulos, M. G.; Luis, J. M.; Kirtman, B. *J. Phys. Chem. A* **2011**, *115*, 10370−10381. (j) Torrent-Sucarrat, M.; Anglada, J. M.; Luis, J. M. *J. Chem. Theory Comput.* **2011**, *7*, 3935−3943. (k) Naves, E. S.; Castro, M. A.; Fonseca, T. L. *J. Chem. Phys.* **2012**, *136*, 014303.

(10) (a) Bishop, D. M.; Kirtman, B. *J. Chem. Phys.* **1991**, *95*, 2646−2658. (b) Bishop, D. M.; Kirtman, B. *J. Chem. Phys.* **1992**, *97*, 5255−5256. (c) Bishop, D. M.; Luis, J. M.; Kirtman, B. *J. Chem. Phys.* **1998**, *108*, 10013−10017.

(11) (a) Bishop, D. M.; Hasan, M.; Kirtman, B. *J. Chem. Phys.* **1995**, *103*, 4157−4159. (b) Luis, J. M.; Duran, M.; Andrés, J. L. *J. Chem. Phys.* **1997**, *107*, 1501−1512. (c) Kirtman, B.; Luis, J. M.; Bishop, D. M. *J. Chem. Phys.* **1998**, *108*, 10008−10012. (d) Luis, J. M.; Martí, J.; Duran, M.; Andrés, J. L.; Kirtman, B. *J. Chem. Phys.* **1998**, *108*, 4123−4130.

(12) (a) Torrent-Sucarrat, M.; Solà, M.; Duran, M.; Luis, J. M.; Kirtman, B. *J. Chem. Phys.* **2002**, *116*, 5363−5373. (b) Torrent-Sucarrat, M.; Solà, M.; Duran, M.; Luis, J. M.; Kirtman, B. *J. Chem. Phys.* **2004**, *120*, 6346−6355.

(13) (a) Torrent-Sucarrat, M.; Luis, J. M.; Kirtman, B. *J. Chem. Phys.* **2005**, *122*, 204108. (b) Christiansen, O.; Kongsted, J.; Paterson, M. J.; Luis, J. M. *J. Chem. Phys.* **2006**, *125*, 214309. (c) Luis, J. M.; Torrent-Sucarrat, M.; Christiansen, O.; Kirtman, B. *J. Chem. Phys.* **2007**, *127*, 084118. (d) Hansen, M. B.; Christiansen, O.; Hattig, C. *J. Chem. Phys.* **2009**, *131*, 154101.

(14) (a) Bishop, D. M.; Dalskov, E. K. *J. Chem. Phys.* **1996**, *104*, 1004−1011. (b) Quinet, O.; Champagne, B. *J. Chem. Phys.* **1998**, *109*, 10594−10602. (c) Luis, J. M.; Duran, M.; Kirtman, B. *J. Chem. Phys.* **2001**, *115*, 4473−4483.

(15) (a) Christiansen, O. *J. Chem. Phys.* **2005**, *122*, 194105. (b) Seidler, P.; Sparta, M.; Christiansen, O. *J. Chem. Phys.* **2011**, *134*, 054119. (c) Hansen, M. B.; Christiansen, O. *J. Chem. Phys.* **2011**, *135*, 154107.

(16) Kirtman, B.; Luis, J. M. *Int. J. Quantum Chem.* **2011**, *111*, 839−847.

(17) Becke, A. D. *J. Chem. Phys.* **1993**, *98*, 5648−5652.

(18) Frisch, M. J.; Trucks, G. W.; Schlegel, H. B.; Scuseria, G. E.; Robb, M. A.; Cheeseman, J. R.; Scalmani, G.; Barone, V.; Mennucci, B.; Petersson, G. A.; Nakatsuji, H.; Caricato, M.; Li, X.; Hratchian, H. P.; Izmaylov, A. F.; Bloino, J.; Zheng, G.; Sonnenberg, J. L.; Hada, M.; Ehara, M.; Toyota, K.; Fukuda, R.; Hasegawa, J.; Ishida, M.; Nakajima, T.; Honda, Y.; Kitao, O.; Nakai, H.; Vreven, T.; Montgomery, J. A., Jr.; Peralta, J. E.; Ogliaro, F.; Bearpark, M.; Heyd, J. J.; Brothers, E.; Kudin, K. N.; Staroverov, V. N.; Kobayashi, R.; Normand, J.; Raghavachari, K.; Rendell, A.; Burant, J. C.; Iyengar, S. S.; Tomasi, J.; Cossi, M.; Rega, N.; Millam, J. M.; Klene, M.; Knox, J. E.; Cross, J. B.; Bakken, V.; Adamo, C.; Jaramillo, J.; Gomperts, R.; Stratmann, R. E.; Yazyev, O.; Austin, A. J.; Cammi, R.; Pomelli, C.; Ochterski, J. W.; Martin, R. L.; Morokuma, K.; Zakrzewski, V. G.; Voth, G. A.; Salvador, P.; Dannenberg, J. J.; Dapprich, S.; Daniels, A. D.; Farkas, Ö.; Foresman, J. B.; Ortiz, J. V.; Cioslowski, J.; Fox, D. J. *Gaussian 09*, revision C.01; Gaussian, Inc.: Wallingford, CT, 2009.

(19) (a) Hehre, W. J.; Ditchfie, R; Pople, J. A. *J. Chem. Phys.* **1972**, *56*, 2257−2261. (b) Dill, J. D.; Pople, J. A. *J. Chem. Phys.* **1975**, *62*, 2921−2923. (c) Krishnan, R.; Binkley, J. S.; Seeger, R.; Pople, J. A. *J. Chem. Phys.* **1980**, *72*, 650−654.

(20) (a) Luis, J. M.; Duran, M.; Champagne, B.; Kirtman, B. *J. Chem. Phys.* **2000**, *113*, 5203−5213. (b) Luis, J. M.; Champagne, B.; Kirtman, B. *Int. J. Quantum Chem.* **2000**, *80*, 471−479.

(21) Luis, J. M.; Duran, M.; Andrés, J. L.; Champagne, B.; Kirtman, B. *J. Chem. Phys.* **1999**, *111*, 875−884.

(22) Eckart, C. *Phys. Rev.* **1926**, *28*, 0711−0726.

(23) Davis, P. J.; ; Rabinowitz, P. In *Numerical Integration*; Blaisdell: London, 1967; pp 166−173.

(24) (a) Champagne, B.; Perpète, E. A.; van Gisbergen, S. J. A.; Baerends, E. J.; Snijders, J. G.; Soubra-Ghaoui, C.; Robins, K. A.; Kirtman, B. *J. Chem. Phys.* **1998**, *109*, 10489−10498. (b) van Gisbergen, S. J. A.; Schipper, P. R. T.; Gritsenko, O. V.; Baerends, E. J.; Snijders, J. G.; Champagne, B.; Kirtman, B. *Phys. Rev. Lett.* **1999**, *83*, 694−697. (c) Champagne, B.; Perpète, E. A.; Jacquemin, D.; van Gisbergen, S. J. A.; Baerends, E. J.; Soubra-Ghaoui, C.; Robins, K. A.; Kirtman, B. *J. Phys. Chem. A* **2000**, *104*, 4755−4763.